Q estimation by a match-filter method

Peng Cheng and Gary F. Margrave

Knowledge of Q is desirable for improving seismic resolution through inverse Q filtering, facilitating amplitude analysis and seismic interpretation, and understanding the subsurface environment better. However, Q is rarely measured since estimates are mainly made from VSP data, which is usually not available. In addition, the question of reliable Q estimation remains, especially in case of unfavorable signal to noise ratio (SNR). Estimating Q from VSP or even reflection data in presence of moderate noise with sufficient accuracy is still under investigation. To address this problem, a match-filter method for Q estimation is proposed in this paper, and evaluated using synthetic 1D, 2D data and field data. Our method takes two local amplitude spectra from different times in a seismic record and estimates the interval Q between them. First we compute minimum-phase equivalent wavelets from each amplitude spectra, and then we find the best forward Q filter that best matches the shallow wavelet to the deeper wavelet. Our method is theoretically similar to the spectral-ratio method because the inverse Fourier transform of a spectral ratio is a matching filter. However, computing the match filter in the time domain is more robust in the presence of noise than direct spectral division in the frequency domain. Testing results show that the proposed method is, compared to the spectral-ratio method, more robust to noise and more suitable for the Q estimation from reflection, and has the potential to indentify a localized low Q zone of the subsurface, which can be used as a gas indicator.

INTRODUCTION

The attenuation of seismic waves is a property of the earth which is quantified by Q, the seismic quality factor. The parameter Q is of great interest to scientists. Firstly, the preferential attenuation of high frequency degrades the seismic resolution. Given knowledge of Q, the resolution can be enhanced by inverse Q filtering or migration methods. Secondly, amplitude analysis for AVO is complicated by Q because the attenuation effects are superimposed on AVO signature. This distortion can be correct if accurate Q values are available. Furthermore, the parameter Q depends on lithology, porosity, and fluid or gas saturation. Therefore, Q can provide important information about the subsurface to facilitate seismic interpretation.

Although the knowledge of Q is very desirable, Q is yet rarely measured. Conventionally, Q is estimated from transmission data, such as VSP data (Hague, 1981; Tonn, 1991), crosswell (Quan and Harris, 1997; Neep et al., 1996) and sonic logging (Sun et al., 2000). There are various methods for Q estimation such as analytical signal method (Engelhard, 1996), spectral-ratio method (Bath, 1974), and the centroid frequency-shift method (Quan and Harris, 1997), and each method has its strength and limit. An extensive comparison between various methods for Q estimation was made by Tonn (1991) using VSP data; and a conclusion was made that the analytical signal method is superior if true amplitude recordings are available and otherwise the spectral-ratio method is optimal in the noise-free case. The estimation given by spectral-ratio method may deteriorate drastically with increasing noise (Patton, 1988; Tonn, 1991). Although transmission data (e.g. VSP) are ideal for Q estimation, they have limited areal

coverage and are more expensive than surface data. Therefore, in practice, it is more useful to estimate Q from the surface reflection data. However, very few publications address the Q estimation using surface seismic data. Dasgupta and Clark (1998) proposed a Q versus offset (QVO) method for estimating Q from surface data, which essentially applied the classic spectral-ratio method on a trace by trace basis to the designatured and NMO corrected CMP gather. For reflection data, Q must be derived from the change in the spectra of reflections. The spectrum of the reflected wave is subjected to the tuning effect (Sheriff and Geldart, 1995) of local thin-bed formation. Hackert and Parra (2004) proposed an approach to remove this tuning effect from the QVO method using reference well log data. Generally, estimating Q from noisy data or surface reflection data needs further investigation.

The purpose of our work is to propose and evaluate a robust method for Q estimation that is suitable for application to reflection data. This paper is organized as follows: the first part introduces the classic spectral-ratio method. Based on that, a match-filter method for Q estimation is developed. Following the above theoretical material, numerical examples will be used to evaluate the proposed match-filter method. Finally, some conclusions are drawn from results of the examples.

THEORY OF MATCH-FILTER METHOD

The theory of the constant Q model for seismic attenuation is well established (Futterman, 1962; Aki and Richards, 1980). Suppose that a seismic wavelet with amplitude spectrum $A_1(f)$ has a amplitude spectrum $A_2(f)$ after traveling in the attenuating media for an interval time t. Then, we have

$$A_2(f) = \mathrm{G}A_1(f)\exp\left(\frac{-\pi f t}{Q}\right), \tag{1}$$

where f is the frequency, G is the geometric spreading factor. More generally, G can represent all the frequency independent energy loss in total, including spherical divergence, reflection and transmission loss. Equation (1) can be rearranged as

$$\ln\left(\frac{A_2(f))}{A_1(f)}\right) = \ln(\mathrm{G}) - \frac{\pi f t}{\mathrm{Q}}. \tag{2}$$

Therefore, the Q factor can be estimated from fitting a straight line to the spectral ratio over a finite frequency range. And Q has a direct relation with the slope k of the linear line as

$$\mathrm{Q} = -\frac{\pi f t}{k}. \tag{3}$$

The above is the basic theory of the classic spectral-ratio method, which is originally derived for use with VSP data. For reflection data, the reflected wave can be approximately regarded as the convolution of the source wavelet with the reflectivity time series. So, the spectrum of localized reflected pulse can be significantly affected by the corresponding local reflectors, which makes estimating Q from surface data difficult. A correction method to this effect was discussed by several publications (Raikes and White, 1984; White, 1992; Hackert and Parra, 2004), which we introduce here. Assume that a source wavelet $s(t)$ with a spectrum $S(f)$ travel through layered earth with a

corresponding reflectivity $r(t)$ in two way time, and $g(t)$ denotes the geometric spreading loss of amplitudes. Then, for an acoustic/elastic medium, the reflected signal $a(t)$ can be given by

$$\mathrm{a}(t) = g(t) \int_{-\infty}^{\infty} s(\tau)\, r(t-\tau) d\tau. \quad (4)$$

Consider a local reflected wave $\mathrm{a}_1(t)$, i.e. a windowed part of $\mathrm{a}(t)$ has the contribution from a corresponding subset of reflectivity, $\mathrm{r}_1(t)$, which is around two way time t_1. From (4), we have

$$\mathrm{a}_1(t) = g(t) \int_{-\infty}^{\infty} s(\tau)\, r_1(t-\tau) d\tau. \quad (5)$$

Then the spectrum of the localized reflected signal $\mathrm{a}_1(t)$ near time t_1 can be approximated by

$$\mathrm{A}_1(f) \approx g(t_1)\mathrm{S(f)R}_1\mathrm{(f)}, \quad (6)$$

where $\mathrm{R}_1\mathrm{(f)}$ is the Fourier transform of $\mathrm{r}_1(t)$. If the attenuation of the layered medium can be described by the constant Q model, equation (6) can be modified as

$$|\mathrm{A}_1(f)| \approx g(t_1)|\mathrm{S(f)}||\mathrm{R}_1\mathrm{(f)}| \exp\left(\frac{-\pi f t_1}{Q}\right). \quad (7)$$

Similarly, for a localized reflected signal $\mathrm{a}_2(t)$ near time t_2 with a corresponding local reflectivity series $\mathrm{r}_2(t)$, its amplitude spectrum can be formulated as

$$|\mathrm{A}_2(f)| \approx g(t_2)|\mathrm{S(f)}||\mathrm{R}_2\mathrm{(f)}| \exp\left(\frac{-\pi f t_2}{Q}\right), \quad (8)$$

where $\mathrm{R}_2\mathrm{(f)}$ is the Fourier transform of $\mathrm{r}_2(t)$. From equation (7) and (8), we have

$$\ln\left(\left|\frac{A_2(f)}{A_1(f)}\right|\right) = \ln\left(\frac{g(t_2)}{g(t_1)}\right) + \ln\left(\left|\frac{R_2(f)}{R_1(f)}\right|\right) - \frac{\pi f(t_2-t_1)}{\mathrm{Q}}. \quad (9)$$

Usually, $\left|\frac{R_2(f))}{R_1(f)}\right|$ varies with frequency, and Q is not proportional to the slope of the logarithm spectral ratio. If well log data available, $\mathrm{r}(t)$ can be calculated from the impedance and, then correction can be made to equation (9) as (Hackert and Parra, 2004)

$$\ln\left(\left|\frac{A_2(f)/R_2(f)}{A_1(f)/R_1(f)}\right|\right) = \ln\left(\frac{g(t_2)}{g(t_1)}\right) - \frac{\pi f(t_2-t_1)}{\mathrm{Q}}. \quad (10)$$

Therefore, Q can be estimated using the spectral-ratio method.

Compare equation (9) with equation (2), we can see that Q can be estimated exactly the same way as the classic spectral-ratio method if $\left|\frac{R_2(f))}{R_1(f)}\right|$ is independent of frequency. From the viewpoint of Q estimation, the VSP data can be taken as a special case of the reflection data when $\mathrm{r}_1(t)$ and $\mathrm{r}_2(t)$ represent single isolated reflectors. So, Q estimation method derived based on equation (7) and (8) should be of more general use.

Q estimation usually needs a spectrum from a short time signal. When the computed spectrum is smooth such as the case for VSP data with high SNR, reliable Q estimation

can be obtained. More often, there are spikes or notches in the spectrum caused by noise or the tuning effect of local reflectors, which causes problems for the Q estimation. In this case, the Q estimation can be deteriorated further when the division of spectra is involved. Therefore, the Q estimation could be more robust when smoothed spectra are employed and the division of spectra is avoided.

A multitaper method for smooth, high resolution spectral estimation was proposed by Thomson (1982), which has been shown to provide low variance estimation with less spectral leakage when applied to seismic data (Park et al., 1987; Neep et al., 1996, Cheng and Margrave, 2009). We will use the multitaper method to compute the spectra of local reflected waves. The Burg method (Claerbourt, 1976) for spectral estimation was also tried but it was found that the estimated result has large spikes when the original signal is band limited. From equation (7) and (8), the smoothed amplitude spectra can be formulated as

$$\overline{|\mathrm{A}_1(f)|} \approx g(t_1)\overline{|\mathrm{S(f)}||\mathrm{R}_1(\mathrm{f})|}\exp\left(\frac{-\pi f t_1}{Q}\right), \tag{11}$$

where the overbar indicates smoothing, and

$$\overline{|\mathrm{A}_2(f)|} \approx g(t_2)\overline{|\mathrm{S(f)}||\mathrm{R}_2(\mathrm{f})|}\exp\left(\frac{-\pi f t_2}{Q}\right). \tag{12}$$

When these smoothed spectra are used to conduct Q estimation by spectral-ratio method, equation (9) is changed to

$$\ln\left(\overline{\left|\frac{A_2(f)}{A_1(f)}\right|}\right) = \ln\left(\frac{g(t_2)}{g(t_1)}\right) + \ln\left(\overline{\left|\frac{R_2(f)}{R_1(f)}\right|}\right) - \frac{\pi f(t_2-t_1)}{\mathrm{Q}}. \tag{13}$$

Generally, Q can be estimated by matching $\overline{|\mathrm{A}_1(f)|}$ with $\overline{|\mathrm{A}_2(f)|}$ in some way, using the constant Q model. One approach can be that $\overline{|\mathrm{A}_1(f)|}$ is modified by varying Q until an optimum approximation to $\overline{|\mathrm{A}_2(f)|}$ is obtained using L1 or L2 norm criteria. Considering that this approach may be significantly affected by some frequency components with large magnitudes, which is usually true for a spectrum computed from a short time signal, we choose to match $\overline{|\mathrm{A}_1(f)|}$ with $\overline{|\mathrm{A}_2(f)|}$ in time domain. First, the minimum phase signals with amplitude spectra $\overline{|\mathrm{A}_1(f)|}$ and $\overline{|\mathrm{A}_2(f)|}$ can be formulated as

$$\mathrm{w}_1(\mathrm{t}) = F^{-1}(\overline{|\mathrm{A}_1(f)|}e^{iH(\ln(\overline{|\mathrm{A}_1(f)|}))}) \tag{14}$$

and

$$\mathrm{w}_2(\mathrm{t}) = F^{-1}(\overline{|\mathrm{A}_2(f)|}e^{iH(\ln(\overline{|\mathrm{A}_2(f)|}))}), \tag{15}$$

where F^{-1} denotes inverse Fourier transform; H denotes Hilbert transform. Then, Q can be estimated by

$$\mathrm{Q}_{\mathrm{est}} = min_Q\|\mathrm{w}_1(\mathrm{t}) * \mathrm{I}(\mathrm{Q},\mathrm{t}) - \mu\mathrm{w}_2(\mathrm{t})\|^2, \tag{16}$$

where $*$ denotes convolution, the minimization is taken over the range of possible Q values; and $\mathrm{I}(\mathrm{Q},\mathrm{t})$ is the impulse wave corresponding to the attenuation function with a quality factor value Q and travel time $(t_2 - t_1)$ and can be formulated as

$$\mathrm{I}(\mathrm{Q},\mathrm{t}) = F^{-1}(\exp\left(\frac{-\pi f(t_2-t_1)}{Q} - \mathrm{iH}(\frac{\pi f(t_2-t_1)}{Q})\right)), \tag{17}$$

μ is a constant scaling factor and can be calculated as

$$\mu = \frac{\int_{-\infty}^{\infty}(\mathrm{w}_1(\mathrm{t}) * \mathrm{I}(\mathrm{Q},\mathrm{t}))\ \mathrm{w}_2(\mathrm{t})\mathrm{dt}}{\int_{-\infty}^{\infty}\mathrm{w}_2{}^2(\mathrm{t})\mathrm{dt}}. \tag{18}$$

The match-filter method we propose in this paper is described by equation (16), in which the optimal Q is found by a direct search over an assumed range of Q values with a particular increment since it is a nonlinear minimization. $\mathrm{w}_1(\mathrm{t})$ and $\mathrm{w}_2(\mathrm{t})$ can be regarded as the embedded wavelets at time t_1 and t_2 respectively. For attenuating media, the embedded wavelet evolves with time. Then, Q can be estimated by fitting the evolution of embedded wavelet to constant Q model. Although the embedded wavelet can be assumed to be of minimum phase, this assumption is not a prerequisite for our match-filter method. As mentioned above, equation (6) can be generally regarded as a way to fit the change of spectra using constant Q model. So, this match filter can be applied to reflection data either before or after deconvolution as long as it is a stationary deconvolution algorithm.

In this paper, the proposed match-filter method will be compared to the spectral-ratio method based on equation (13). Often, the calculated spectral ratios are not suitable for linear line fitting over a wide frequency band because of effects outside the simple Q model, and a narrow frequency band should be employed instead, which may be chosen interpretively case by case. To address this problem, the spectral ratios are approximated by polynomial curves, then the local slopes can be derived from the first order derivative of the curve. Finally, Q can be estimated from a medium or mean value of the local slopes. This approach is actually a piecewise linear-line fitting instead of single straight line fitting scheme compared to the original scheme. We call this approach the modified spectral-ratio method in this paper.

NUMERICAL TEST

Synthetic 1D VSP data or reflection data with isolated reflectors

The ideal test for Q estimation is computing Q from noise free VSP data, which can be used to validate Q estimation methods theoretically. A synthetic attenuated seismic trace was created by a nonstationary convolution model proposed by Margrave (1998), using two isolated reflectors, a minimum phase wavelet with dominant frequency of 40 Hz and a constant Q value of 80, as shown in figure 1. Using the two local events in figure 1, Q estimations from the spectral-ratio method and the match-filter method are shown in figure 2 and 3 respectively. Figure 4 shows the fitting error of different Q values for the match-filter method. We can see that both methods give accurate estimations.

Random noise is added to the synthetic data to evaluate the performance of the Q estimation methods. Figure 5 shows a synthetic seismic trace with a noise level of SNR=4. The amplitude spectra of the two events are show in figure 6 and figure 7, which have a moderate noise level of -25 DB and -18 DB respectively. The Q estimations by the spectral-ratio method and the match-filter method are shown in figure 8 and figure 9. For the spectral-ratio method, the straight line fitting is conducted from 15 Hz to 75Hz.

For the match-filter method, a band-pass filter is applied before estimating the embedded wavelets using equation (14) and (15). And the smoothing of amplitude spectra is not conducted at this time. We can see that the Q estimation is deviated from the exact Q value because of the noise. To further evaluate the two Q estimation methods in presence of noise, 200 seismic traces are created by adding 200 difference random noise series of the same level (SNR=4) to the trace shown in figure 1. Then Q estimation is conducted using these noisy data. The histograms of the estimated Q values are shown in figure 10 and 11. We can see that result of match-filter method is better than that of spectral method with a closer mean value of 80.09 and a smaller standard deviation value. Then, the multitaper method is employed to smooth the spectrum for the match-filter method, and Q estimation is conducted using 200 seismic traces, similar to the one show in figure5, with a noise level of SNR = 4. As shown in figure 12, the estimated Q values have a mean value of 78.72 that is still close to 80, and a significantly smaller standard deviation value of 5.68, which is much better than the result shown in figure 10. Next, the case of extensive noise is used to evaluate the match-filter method. The Q estimation is conducted using 200 seismic traces with a noise level of SNR = 2. AS shown in figure 13, the spectral-ratio method corrupts and gives estimation results with a mean value of 90.14 and standard deviation of 50.10. However, the match-filter method, as shown in figure 14, still gives good estimation with a mean value of 79.58 and standard deviation of 12.03. Therefore, the proposed match-filter method gives accurate estimation and is robust to noise.

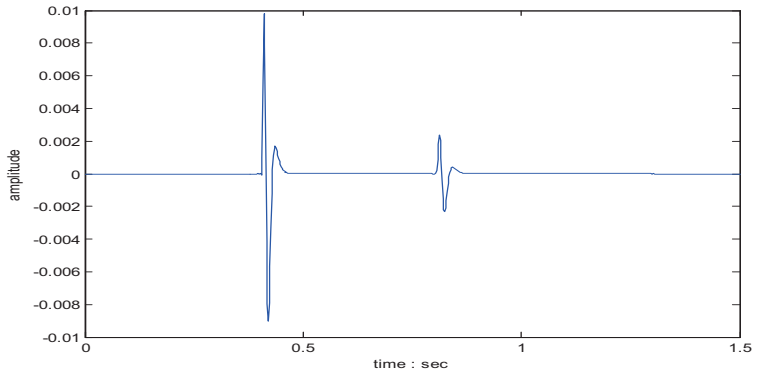

Figure 1. Synthetic seismic trace created with two events, created using two isolated reflectors, a minimum phase source wavelet with dominant frequency of 40 Hz, and a constant Q value of 80.

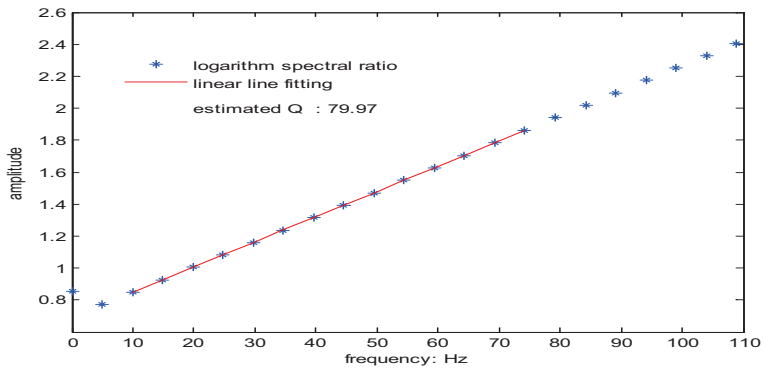

Figure 2. Q estimation by the spectral-ratio method using the two local events shown in figure 1.

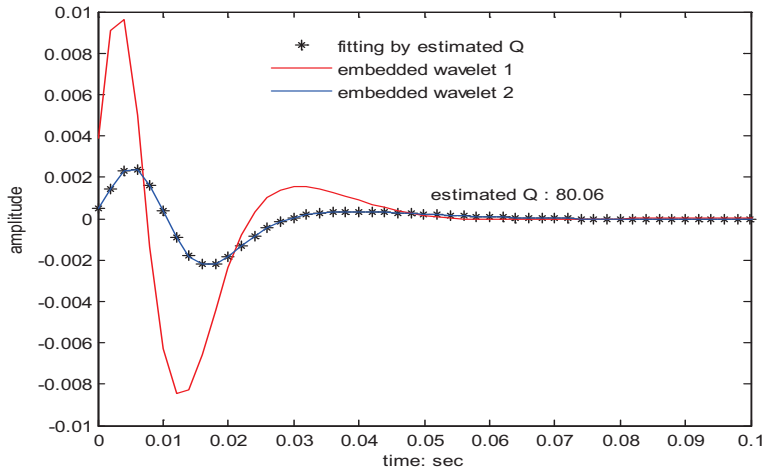

Figure 3. Q estimation by the match-filter method using the two local events shown in figure 1.

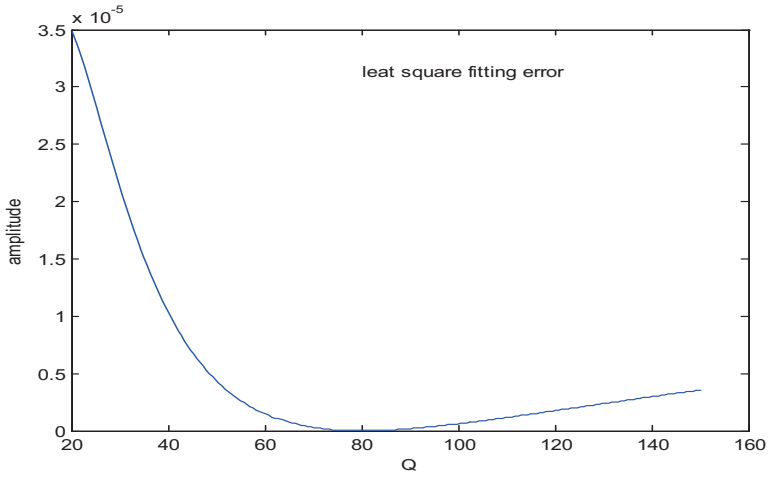

Figure 4. The fitting error curve for Q estimation by the match-filter method corresponding to figure 3

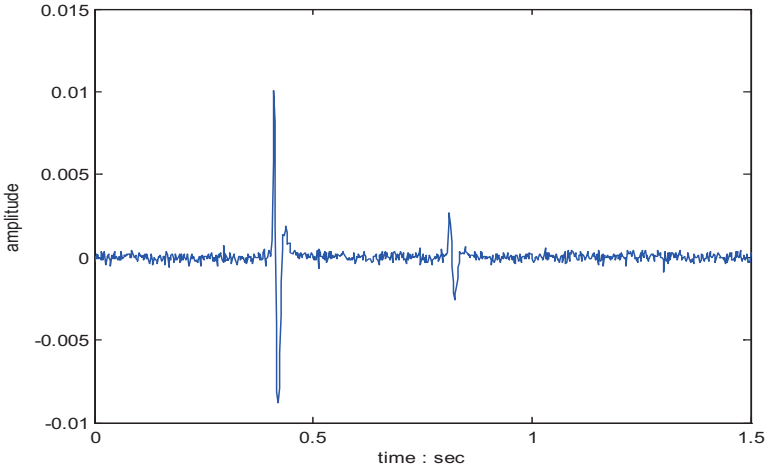

Figure 5. Synthetic seismic trace with noise, created by adding random noise to the seismic trace in figure 1 with SNR=4

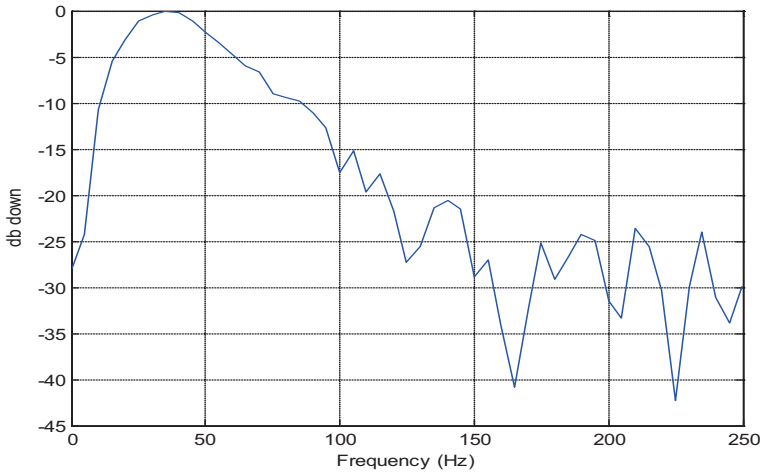

Figure 6. Amplitude spectrum of the local events (0.34s-0.54s) in figure 5

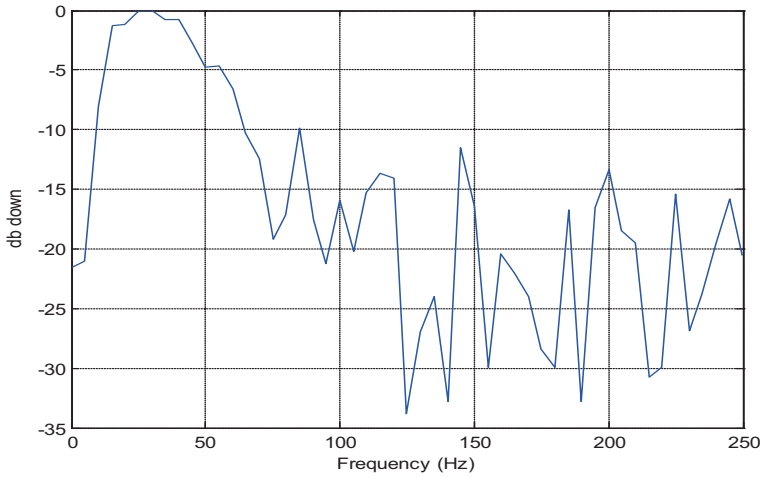

Figure 7. Amplitude spectrum of the events (0.74s-0.94s) second in figure.

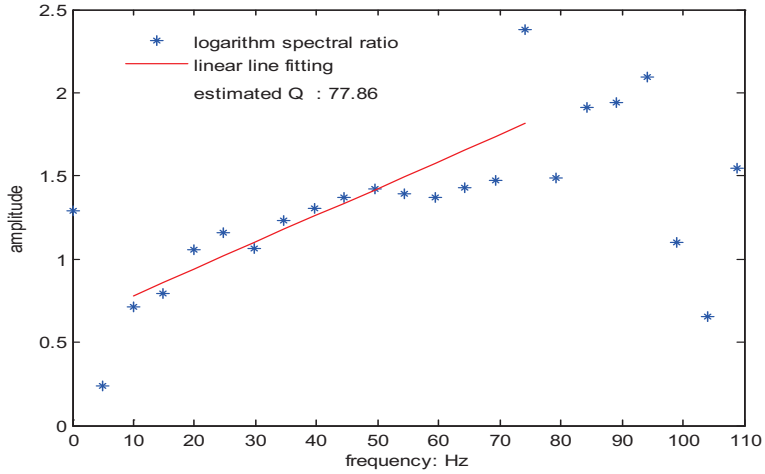

Figure 8. Q estimation by the spectral-ratio method using the two local events shown in figure 5.

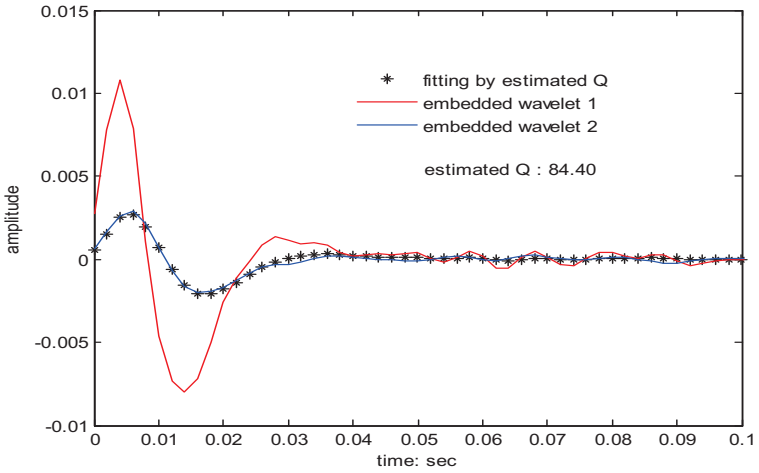

Figure 9. Q estimation by the match-filter method using the two local events shown in figure 5.

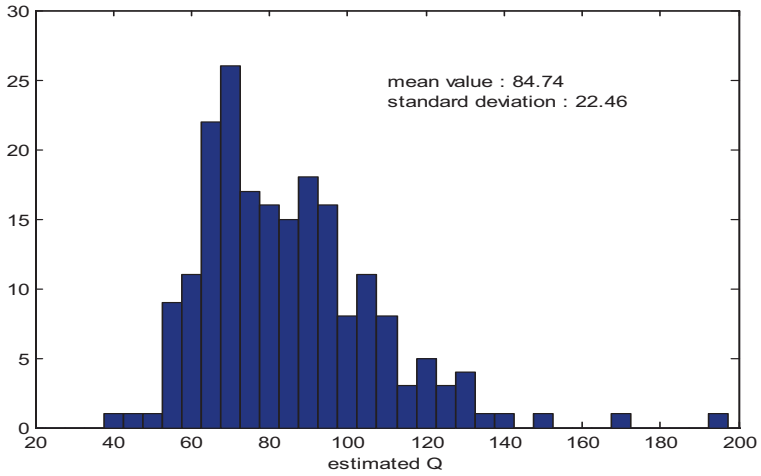

Figure 10. Histogram of the Q values estimated by the spectral-ratio method using 200 seismic trace (similar to the one shown in figure 5) with noise level of SNR=4.

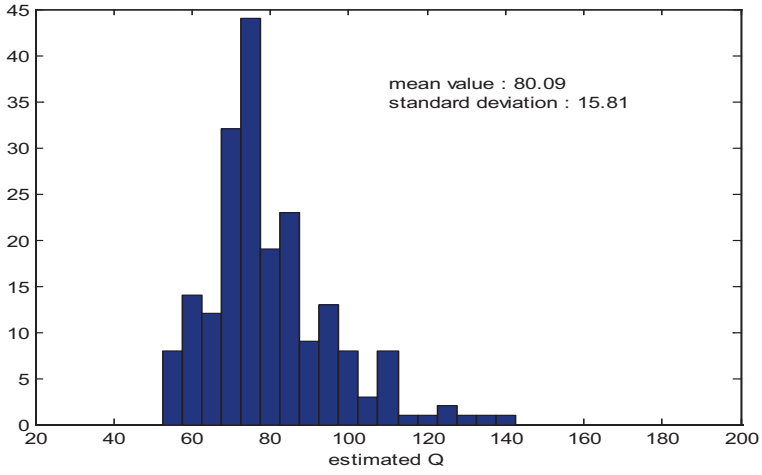

Figure 11. Histogram of the Q values estimated by the match-filter method using 200 seismic trace (similar to the one shown in figure 5) with noise level of SNR=4.

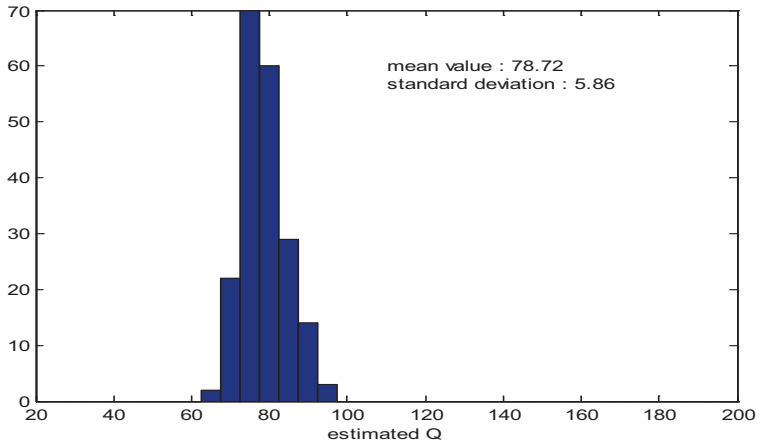

Figure 12. Histogram of the Q values estimated by the match-filter method using 200 seismic trace (similar to the one shown in figure 5) with noise level of SNR=4 (Multitaper method for spectrum estimation is employed).

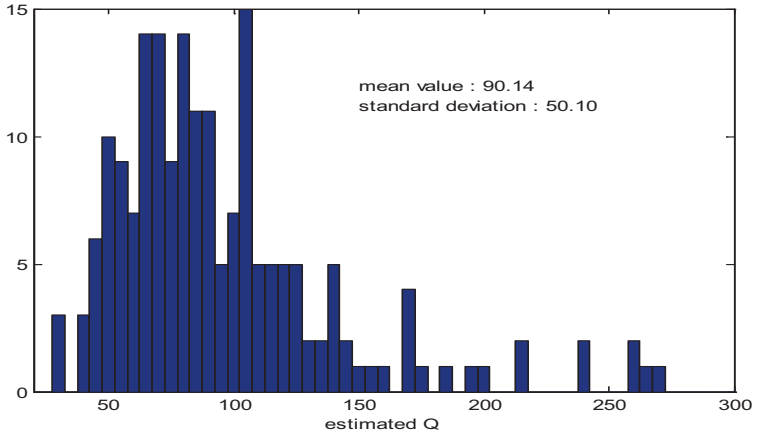

Figure 13. Histogram of the Q values estimated by the spectral-ratio method using 200 seismic trace (similar to the one shown in figure 5) with noise level of SNR=2.

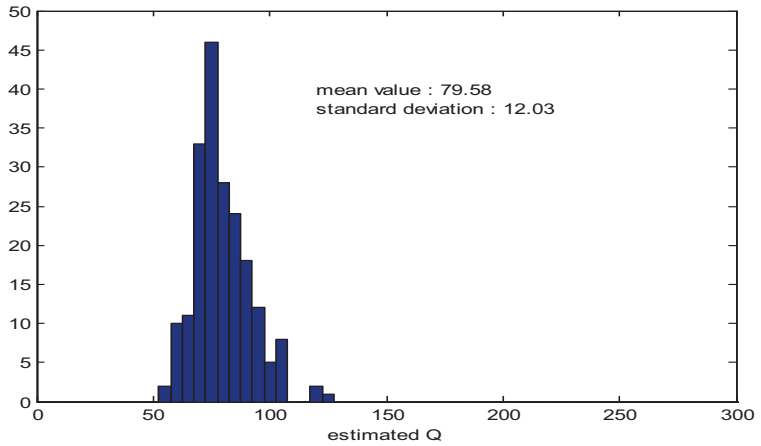

Figure 14. Histogram of the Q values estimated by the match-filter method using 200 seismic trace (similar to the one shown in figure 5) with noise level of SNR=2 (Multitaper method for spectrum estimation is employed).

Synthetic 1D reflection data

Surface reflection data is the most common seismic data so that it is worthwhile to attempt to estimate Q from it. A synthetic seismic trace is created using a random reflectivity series, a minimum phase source wavelet with dominant frequency of 40Hz and a constant Q of 80, as shown in figure 15. Two local reflected waves are obtained by applying time gates of 100ms-500ms and 900ms-1300ms to the attenuated seismic trace, whose amplitude spectra and corresponding smoothed ones are shown in figure 16. The spikes and notches in the original spectra of local reflected waves are obvious, which are mitigated by smoothing using the multitaper method. Q estimation is conducted using the obtained local reflected waves, and the results are shown in figure 17 and 18. Then, attenuated seismic are created using 200 random reflectivity series, from which 200 pairs of local reflected waves are obtained to conduct the Q estimation experiment using the two Q estimations. The results are shown in figure 19 and 20 respectively. We can see that the match-filter method gives better result with closer mean value of 78.00 and smaller standard deviation of 15.17. Next, the two Q estimation methods are further evaluated using reflection date with noise level of SNR=4 and SNR=2. The corresponding results are shown in figure 21- 24. We can see that the spectral-ratio method gives unreliable results with distorted mean value and large standard deviation value, while the match-filter method is insensitive to noise and gives good estimation results for both cases.

At this occasion, the spectral-ratio method corrupts for two reasons. Firstly, even using the smoothed spectra, spectral ratio is sensitive to the spectrum modification caused by noise and the tuning effect of local reflectors. Secondly, the calculated spectral ratios are not suitable for linear line fitting over a wide frequency band anymore. The modified spectral-ratio method mentioned in this paper is more suitable than the original spectral-ratio method. Figure 25 and 26 demonstrate the Q estimation by these two spectral-ratio methods, using one pair of local reflected waves with noise level of SNR=2 as an example. The Q estimation by the modified spectral-ratio method is conducted using the 200 pairs of local reflected waves at different noise level are shown in figure 27 and 28. Compared to the results of spectral-ratio method shown in figure 21 and 23, the Q estimation is improved but still has large standard deviation value.

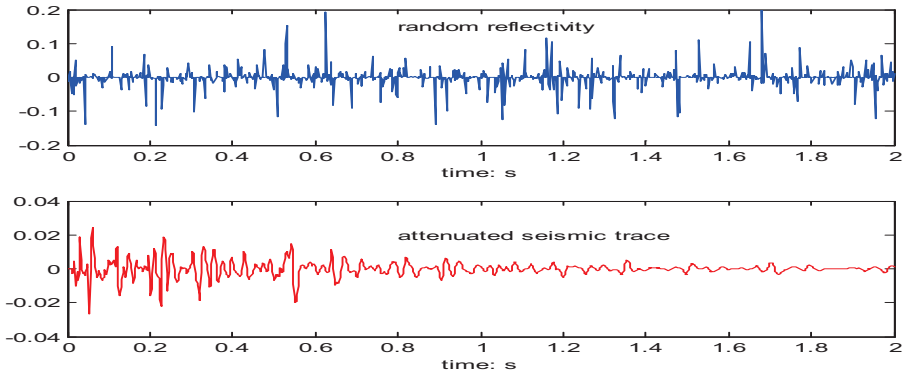

Figure 15. A random reflectivity series (upper). A attenuated seismic trace created using the reflectivity series, a minimum phase wavelet with dominant frequency of 40Hz and a constant Q of 80.

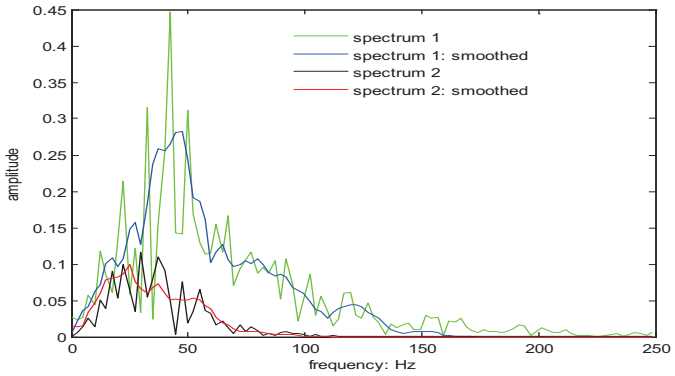

Figure 16. Amplitude spectrum of the 100ms-500ms part of the seismic trace in figure 15 (Green). Amplitude spectrum estimated by multitaper method for the 100ms-500ms part of the seismic trace in figure 15 (Blue). Amplitude spectrum of the 900ms-1300ms part of the seismic trace in figure 15 (Black). Amplitude spectrum estimated by multitaper method for the 900ms-1300ms part of the seismic trace in figure 15 (Red).

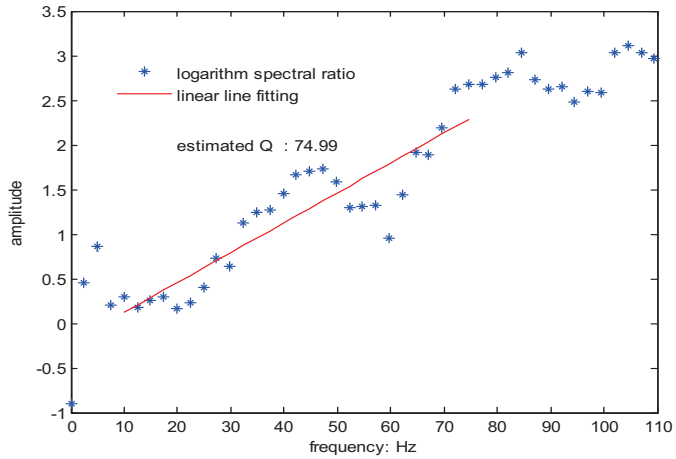

Figure 17. Q estimation by the spectral-ratio method using the 100ms-500ms and 900ms-1300ms parts of the seismic trace shown in figure 15.

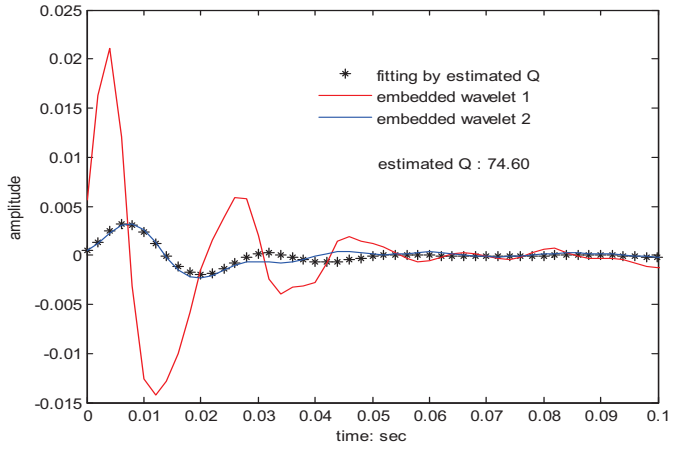

Figure 18. Q estimation by the match-filter method using the 100ms-500ms and 900ms-1300ms parts of the seismic trace shown in figure 15.

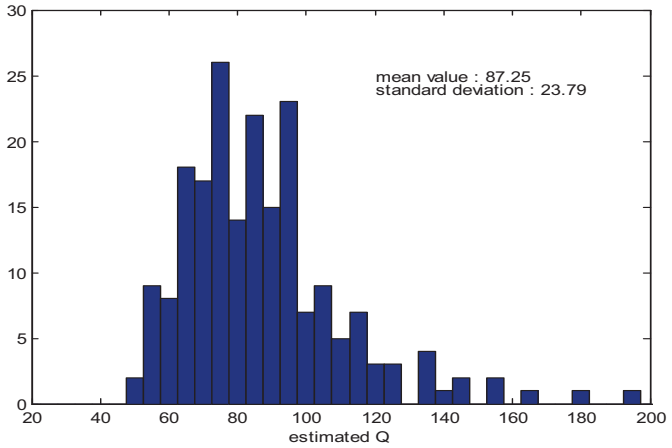

Figure 19. Histogram of the Q values estimated by the spectral-ratio method using the 100ms-500ms and 900ms-1300ms parts of 200 seismic traces which are similar to the one shown in figure 15.

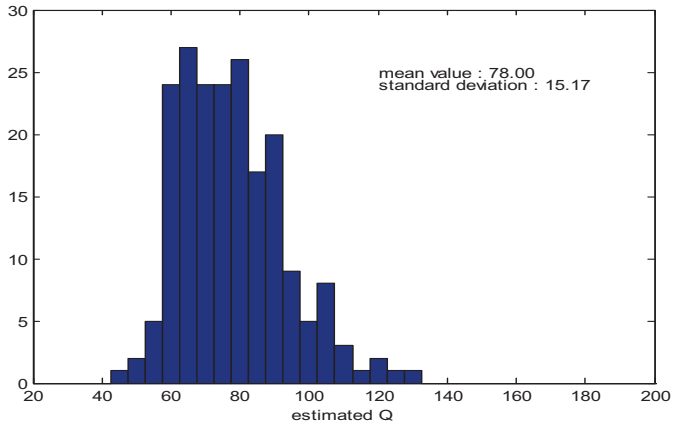

Figure 20. Histogram of the Q values estimated by the match-filter method using the 100ms-500ms and 900ms-1300ms parts of 200 seismic traces which are similar to the one shown in figure 15.

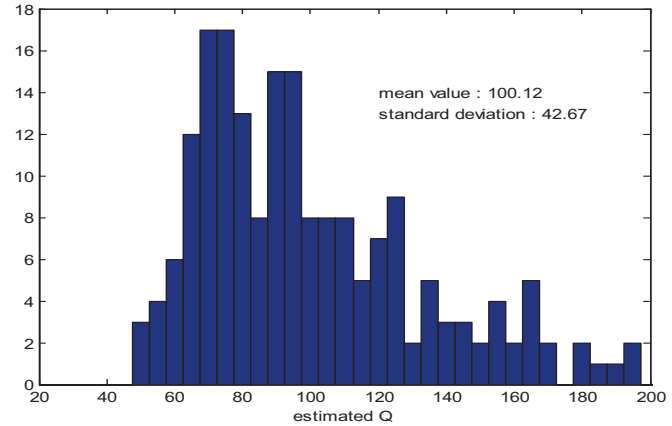

Figure 21. Histogram of the Q values estimated by the spectral-ratio method using the 100ms-500ms and 900ms-1300ms parts of 200 seismic traces with noise level of SNR=4 which are similar to the one shown in figure 15.

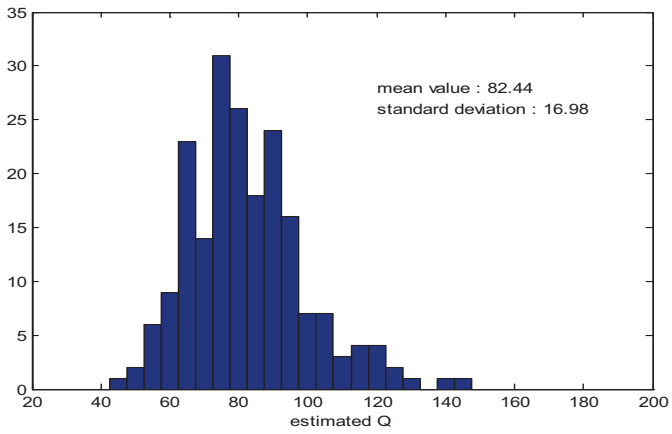

Figure 22. Histogram of the Q values estimated by the match-filter method using the 100ms-500ms and 900ms-1300ms parts of 200 seismic traces with noise level of SNR=4 which are similar to the one shown in figure 15.

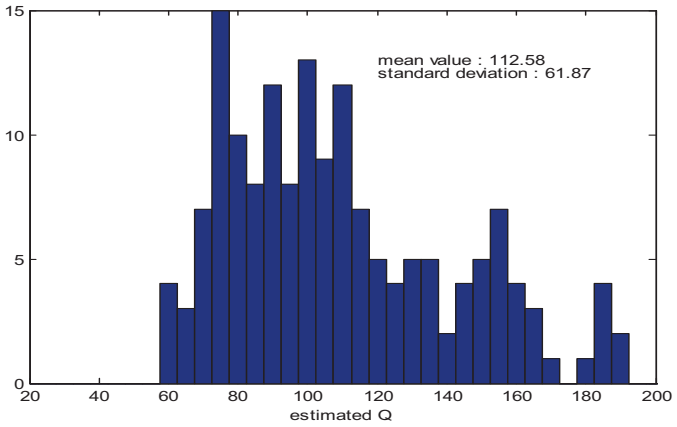

Figure 23. Histogram of the Q values estimated by the spectral-ratio method using the 100ms-500ms and 900ms-1300ms parts of 200 seismic traces with noise level of SNR=2 which are similar to the one shown in figure 15.

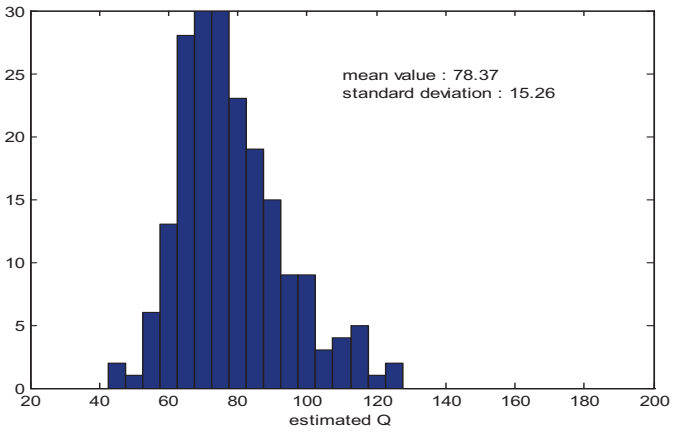

Figure 24. Histogram of the Q values estimated by the match-filter method using the 100ms-500ms and 900ms-1300ms parts of 200 seismic traces with noise level of SNR=4 which are similar to the one shown in figure 15.

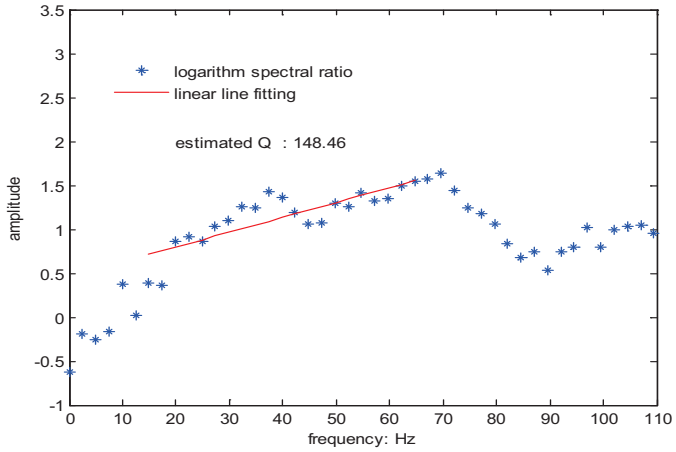

Figure 25. Q estimation by the spectral-ratio method using the 100ms-500ms and 900ms-1300ms parts of a seismic traces with noise level of SNR=4 which is similar to the one shown in figure 15.

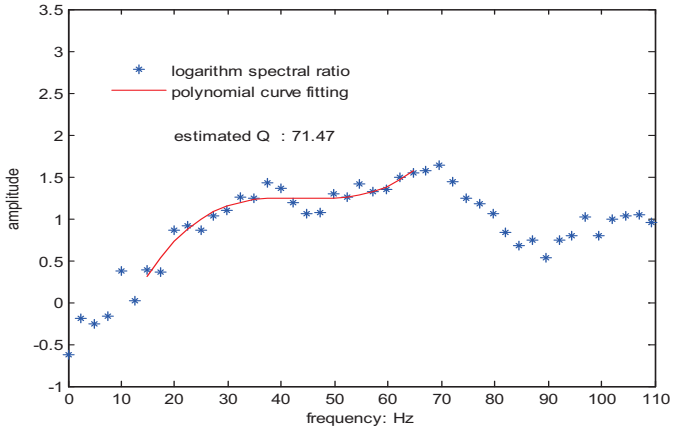

Figure 26. Q estimation by the modified spectral-ratio method using the 100ms-500ms and 900ms-1300ms parts of a seismic traces with noise level of SNR=4 which is similar to the one shown in figure 15.

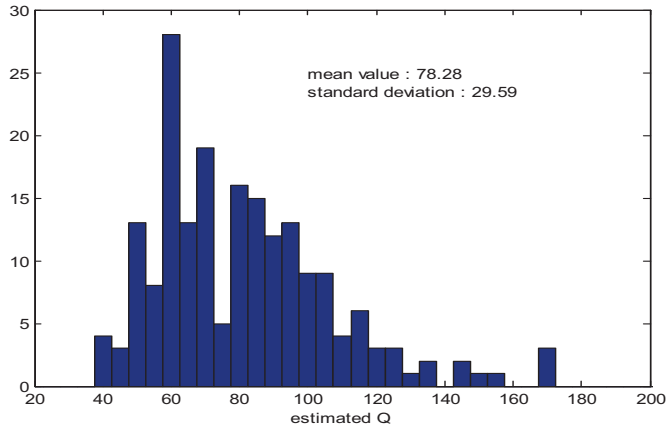

Figure 27. Histogram of the Q values estimated by the modified spectral-ratio method using the 100ms-500ms and 900ms-1300ms parts of 200 seismic traces with noise level of SNR=4 which are similar to the one shown in figure 15.

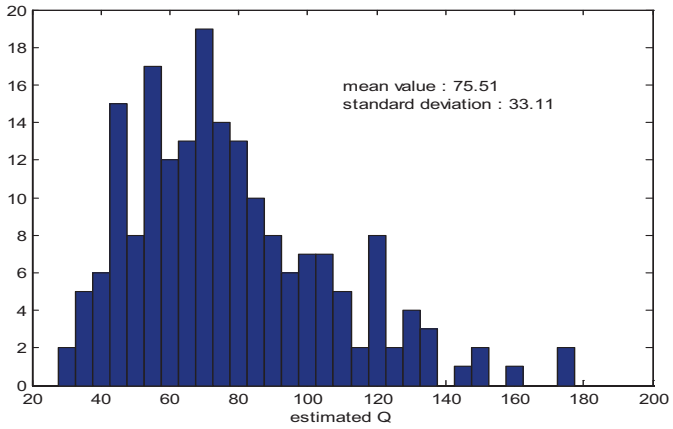

Figure 28. Histogram of the Q values estimated by the modified spectral-ratio method using the 100ms-500ms and 900ms-1300ms parts of 200 seismic traces with noise level of SNR=2 which are similar to the one shown in figure 15.

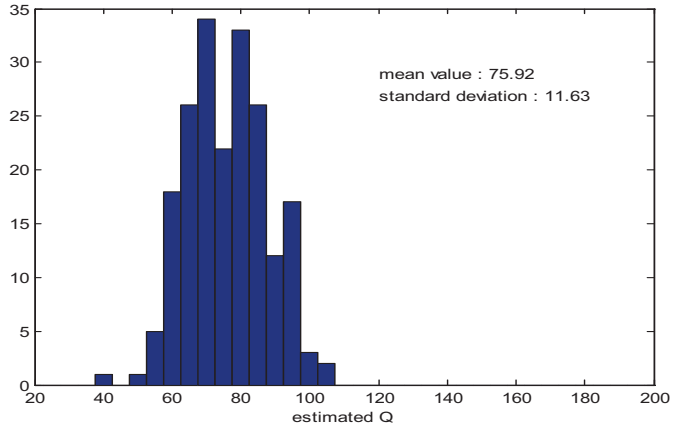

Figure 29. Histogram of the Q values estimated by the match-filter method using the 100ms-500ms and 900ms-1300ms parts of 200 deconvolved seismic traces which are similar to the one shown in figure 15.

To evaluate the effect of deconvolution on Q estimation, the match-filter method is tested using the 200 pairs of local reflected waves after wiener spiking deconvolution. As shown in figure 29, the results are similar to the case without deconvolution shown in figure 20, and have a smaller standard deviation value.

Synthetic 2D data

An important application of Q estimation is that the estimation result can be used as a gas indicator in conjunction with other observation such as flat spot, bright spots, and AVO anomalies. The value of Q drops drastically in presence of gas so that the gas reservoir behaves like a localized low Q zone in the subsurface. Synthetic data for a layered earth model with a low Q zone is used to test the match-filter method, which is created from the seismic modeling using the Tiger software of SINTEF. Figure 30 shows the reflectivity coefficients for layered earth model in two way time. To simplify the computation of travel time, we use an earth model with a constant velocity and layered density structure which is calculated from the random reflectivity coefficients, as

shown in figure 31. The associated Q model is shown in figure 32. The low Q zone has an extension of 1.2s – 1.26s in two-way travel time and 500m -750m in horizontal coordinate. Three shot records corresponding to different source locations of the layered earth model are shown in figure 33, 34 and 35.

To indentify the low Q zone, two time windows with a fixed small interval slide along a seismic trace to obtain pairs of localized reflected waves. For each pair of them, a Q value can be estimated and attributed to the time centered between the two time windows, and the Q estimation is applied to the entire 2D seismic gather trace by trace. Through this approach, a Q profile can be obtained corresponding to the 2D seismic gather. Since the interval time involved with Q estimation is small, the attenuation between the two local reflected waves is usually not obvious except that the latter one travels through the low Q zone and the former one does not. Therefore, the low Q zone in the Q model will cause a relatively low amplitude area in the estimated Q profile. A pair of time windows with a length of 200ms and an interval of 100ms are used to sample the seismic traces. The estimated Q profiles for the three shot records are shown in figure 36, 37 and 38 respectively. We can see that there is hyperbolic distribution of estimated Q values, and the low amplitude area shifts with the varying source locations. Then three NMO corrected CDP gathers are obtained from the shot records with a NMO stretch limit of 30%. The Q profiles of the three CDP gathers are shown in figure 39, 40 and 41. We can see that the hyperbolic distribution of estimated Q values are flattened, and the locations of low amplitude areas in the three Q profiles are corrected and consistent with each other, which match with the low Q zone of the Q model outlined by a rectangle area very well. To refine the low amplitude areas of the Q profiles, the variations of the mean value of Q with travel time or depth and horizontal position are derived from the zoomed low Q areas in figure 39 – 41. From figure 42 and figure 43, the estimated low Q zone should be the areas with a two-way travel time centered at 1.23s and horizontal extension from about 500m to 750m, which is very good math to the Q model. Therefore, the match-filter method has the potential to indentify the low Q zone of 2D seismic data for a layered medium.

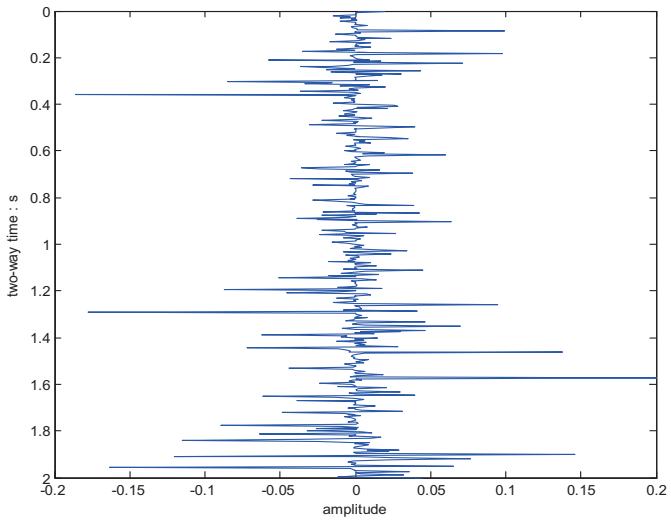

Figure 30. Reflectivity coefficients in two-way travel time for a layered earth model.

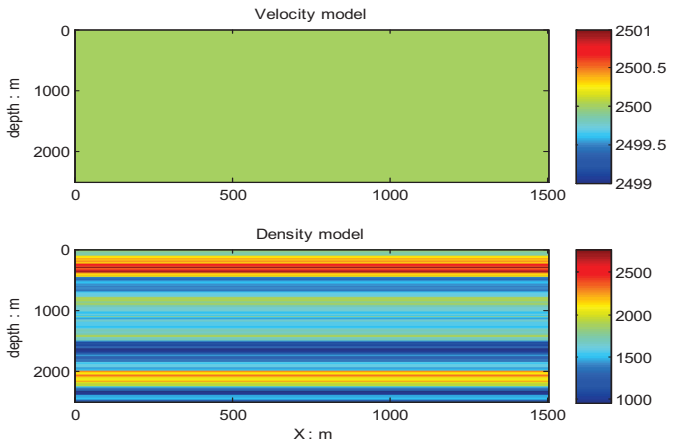

Figure 31. Velocity and density structure for a layered earth model which has the reflectivity coefficients shown in figure 30.

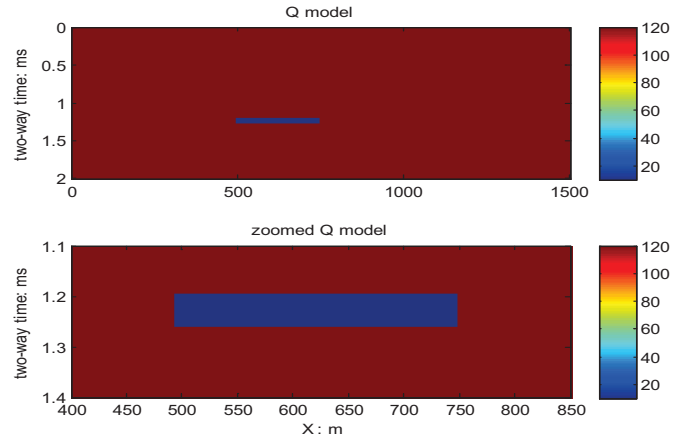

Figure 32. Q model for the layered earth model shown in figure 31.

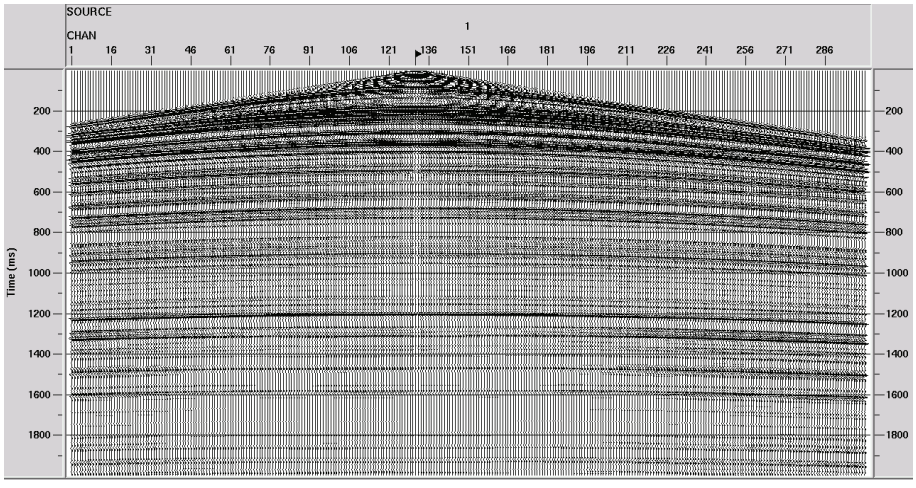

Figure 33. Shot record (geometric spreading compensated) for a layered earth model with velocity and density structure shown in figure 31, Q attenuation structure shown in figure 32; source location (x, z)=(650m, 0m), receiver interval: 5m.

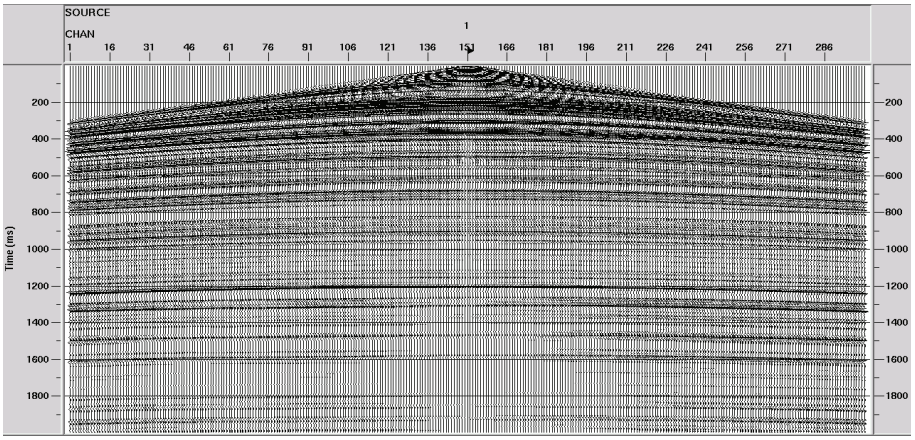

Figure 34. Shot record (geometric spreading compensated) for a layered earth model with velocity and density structure shown in figure 31, Q attenuation structure shown in figure 32; source location (x, z)=(750m, 0m), receiver interval: 5m.

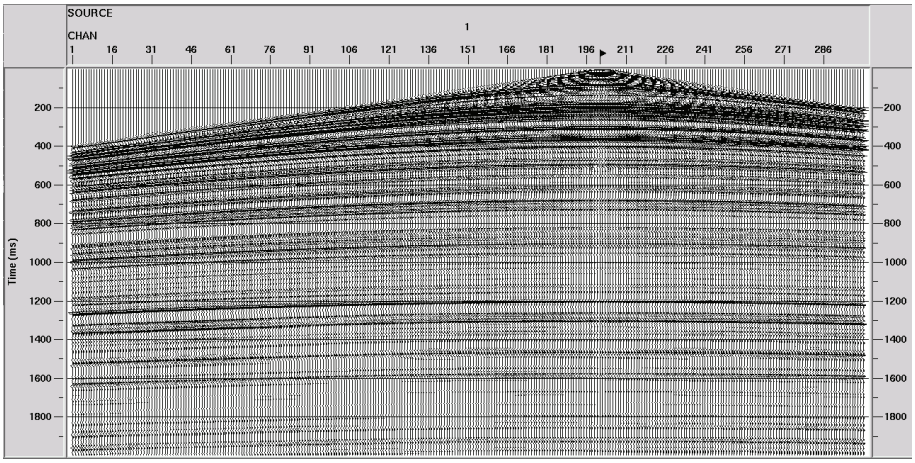

Figure 35. Shot record (geometric spreading compensated) for a layered earth model with velocity and density structure shown in figure 31, Q attenuation structure shown in figure 32; source location (x, z)=(1000m, 0m), receiver interval: 5m

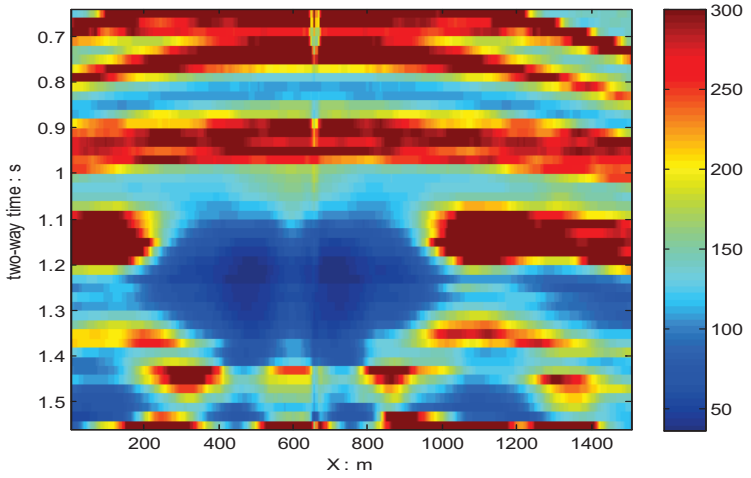

Figure 36. Q profile estimated by the match-filter method using the shot record shown in figure 33.

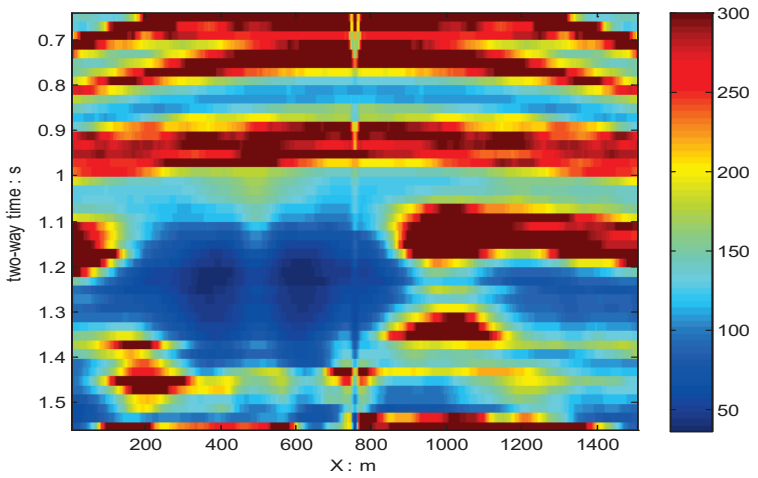

Figure 37. Q profile estimated by the match-filter method using the shot record shown in figure 34.

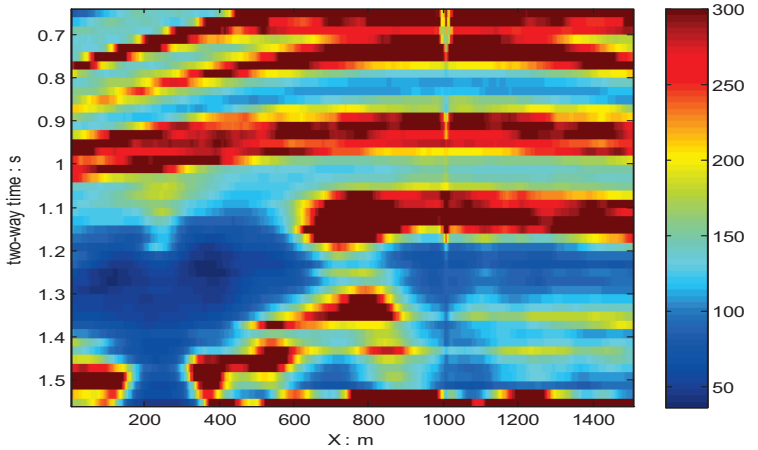

Figure 38. Q profile estimated by the match-filter method using the shot record shown in figure 35.

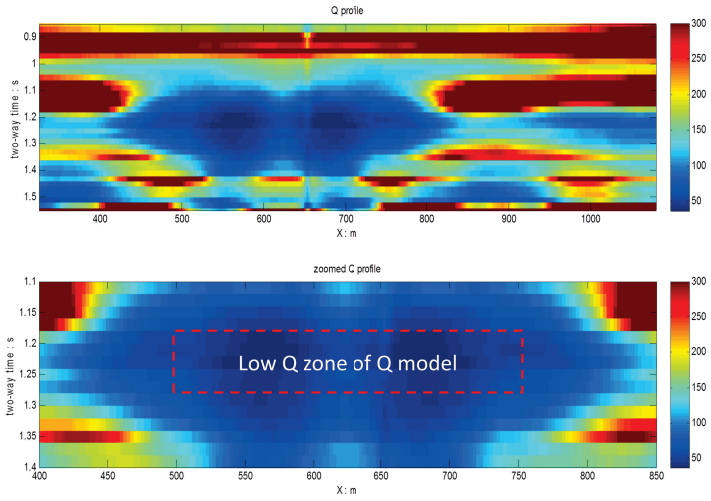

Figure 39. Q profile estimated by the match-filter method using the NMO corrected CDP gather corresponding to the shot record shown in figure 33.

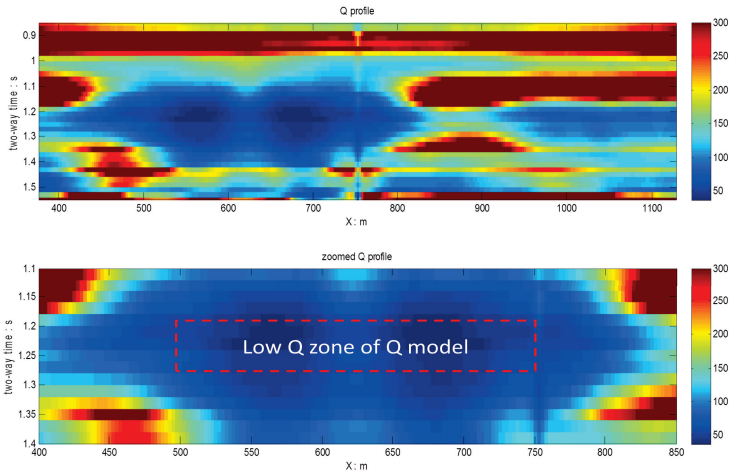

Figure 40. Q profile estimated by the match-filter method using the NMO corrected CDP gather corresponding to the shot record shown in figure 34.

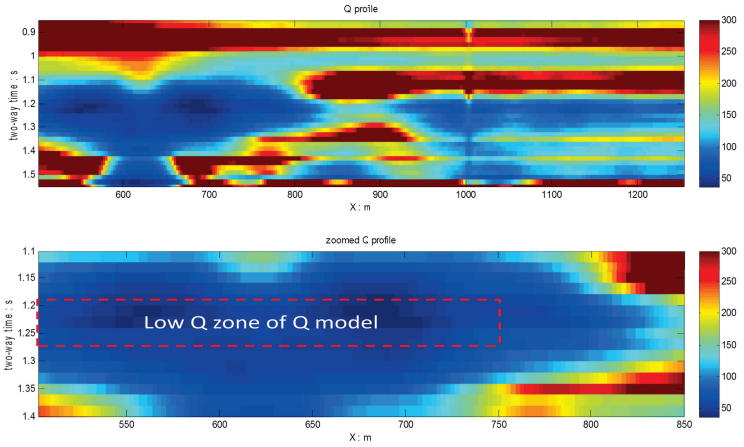

Figure 41. Q profile estimated by the match-filter method using the NMO corrected CDP gather corresponding to the shot record shown in figure 35.

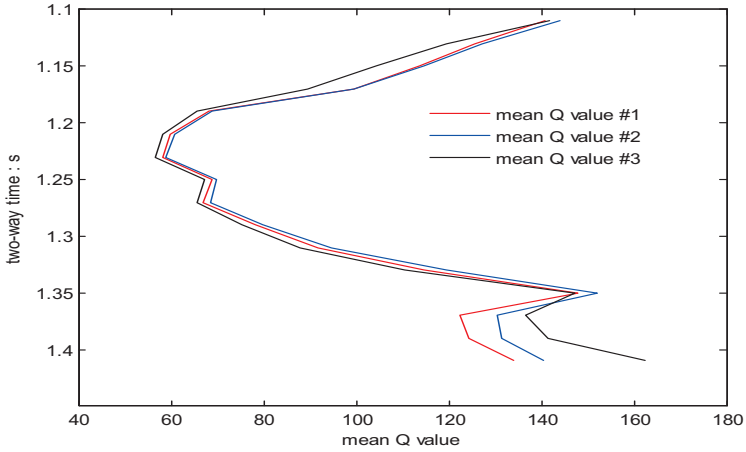

Figure 42. The variation of mean Q value with travel time for the zoomed Q profiles (#1, #2, #3 – the zoomed Q profiles shown in figure 39, 40, 41 respectively).

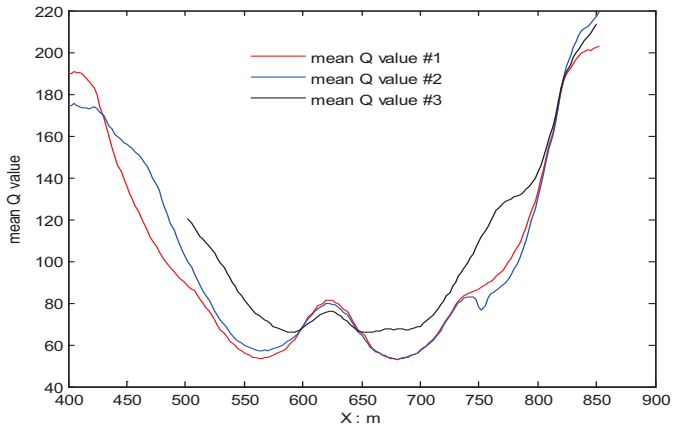

Figure 43. The variation of mean Q value with horizontal coordinates for the zoomed Q profiles (#1, #2, #3 – the zoomed Q profiles shown in figure 39, 40, 41 respectively).

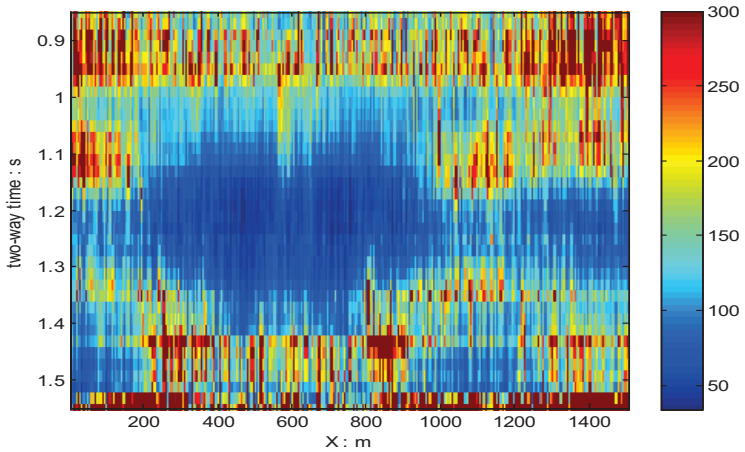

Figure 44. Q profile estimated by the match-filter method using the NMO corrected CDP gather with noise level of SNR=3 corresponding to the shot record shown in figure 33.

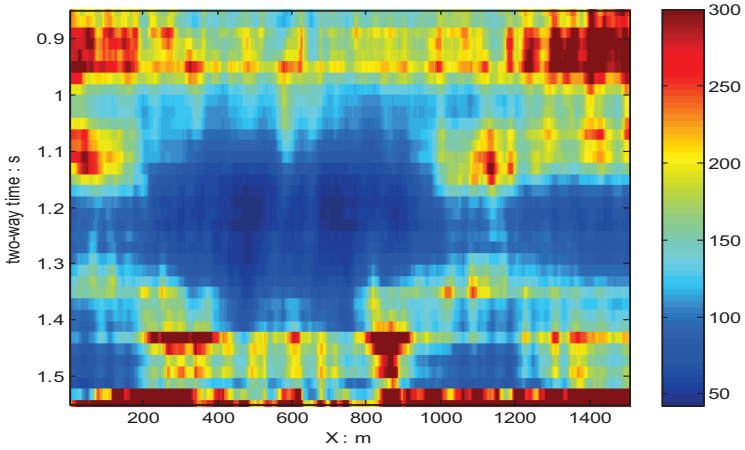

Figure 45. Q profile estimated by the match-filter method using the NMO corrected CDP gather with noise level of SNR=3 corresponding to the shot record shown in figure 33 (An ensemble of neighboring trace are used for spectrum estimation).

To simulate the Q profile estimation for real data, random noise of level SNR=3 is added to the NMO applied CDP gather corresponding to the shot record in figure 33. Then, a Q profile is estimated from the noisy CDP gather. As shown in figure 44, the Q profile is disturbed by noise. To address this problem, the spectrum of local reflected wave can be estimated from a small ensemble of neighboring traces. First, the smoothed spectrum is computed for each trace. Then, the smoothed spectra of an ensemble is scaled and summed using some weighting scheme to give the final spectrum estimation for the trace centered in this ensemble. Adopting this approach of spectrum estimation, Q profile for the noisy CDP gather is computed and shown in figure 45. We can see that the affect of noise is suppressed and the result is similar to the noise free case shown in figure 39.

Real data example

The field data of a 2D seismic line are used to test the match-filter method, which were acquired over the Blackfoot field near Strathmore, Alberta in 1995. The field data were processed using ProMAX software with a job flow including geometric spreading correction, statics correction, predictive deconvolution, NMO correction, trace equalization and stacking. Considering that spectra for the near-offset traces and far-offset traces can be distorted by strong ground rolls and large NMO stretches respectively, the traces with moderate offsets are chosen to conduct the stacking. The stacked data are displayed in CDP bin number, as shown in figure 46. For the Blackfoot line, the target zone is around 1050ms in two-way travel time. In addition, there is a Well 14-09 about 200m away from it, which has nearly the same X coordinate with the trace CDP 36 shown in figure 46.

Q estimation by the match-filter method is conducted using the 750ms-1050ms and 1300-1600ms parts of the traces CDP 25- CDP 265, which roughly gives the average Q for the time interval 900ms-1450ms. The variation of estimated Q values with x coordinates (CDP bin numbers) is shown in figure 47, and the histogram of the estimated Q values is shown in figure 48. We can see that the estimated Q values vary with the trace positions while they remain within a reasonable range. As shown in figure 49, a Q profile was estimated from the CDP gather, using sliding windows with a length of 300ms and an interval of 100ms. We can see that, there is measurable attenuation around 1050ms nearly across the entire line even a small interval time is employed, and the target zone of the well 14-09 locates within the low amplitude area of the estimated Q profile.

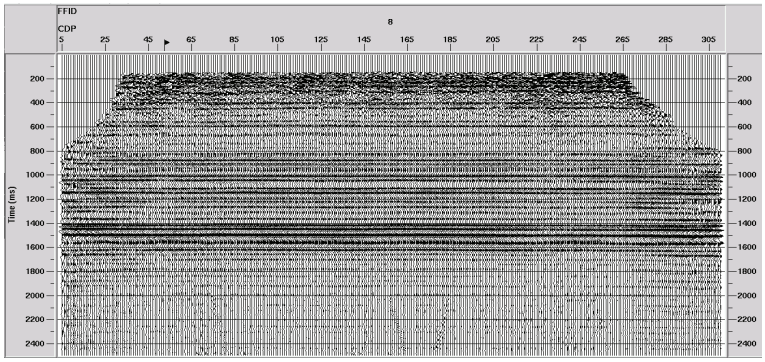

Figure 46 Stacked CDP gather for Blackfoot field data.

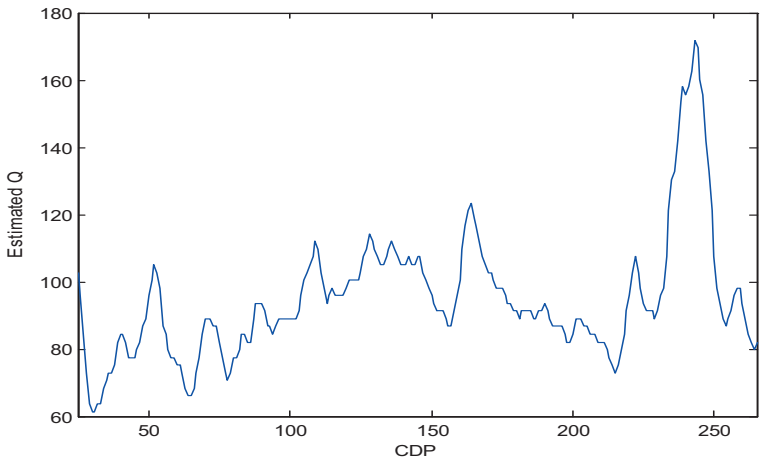

Figure 47. Q values estimated by the match-filter method for the traces CDP 25-265 using their 750ms-1050ms and 1300-1600ms parts.

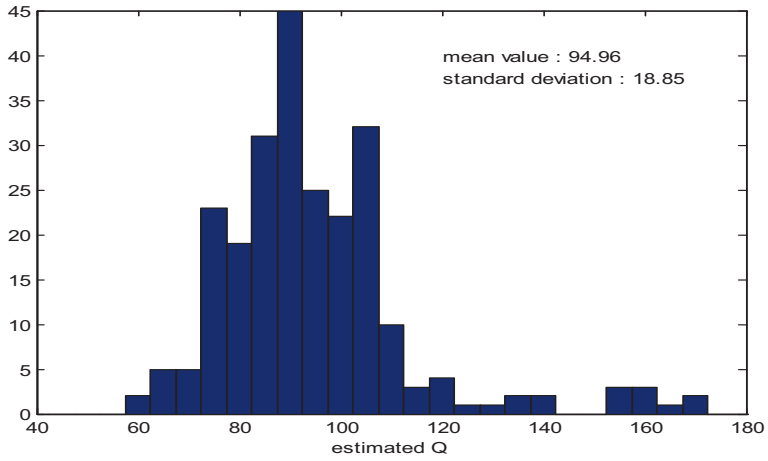

Figure 48. Histogram of the estimated Q values shown in figure 47.

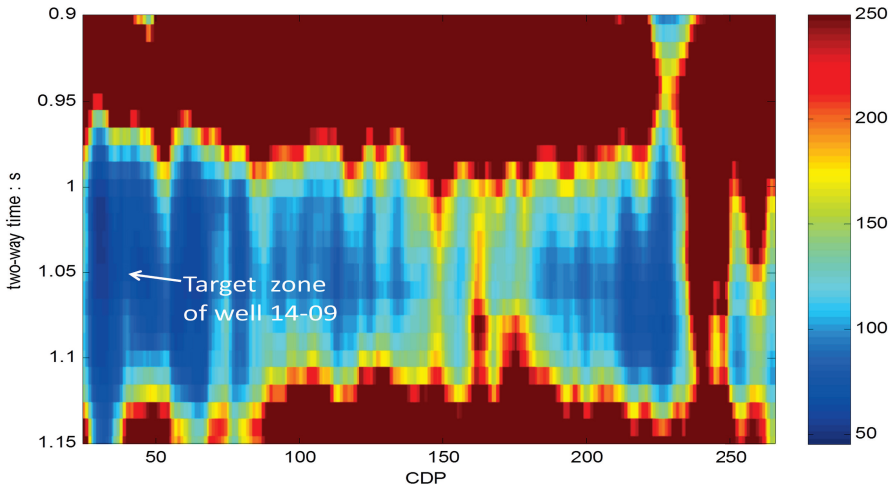

Figure 49. Q profile estimated by the match-filter method for CDP gather shown in figure 46, using sliding windows with a length of 300ms and an interval of 100ms.

CONCLUSION

A match-filter method for Q estimation is proposed and evaluated in this paper. Testing on synthetic seismic trace shows that the proposed match-filter method, compared to the classic spectral-ratio method, gives is robust to noise and more suitable to be applied to reflection data. The match-filter method can be applied to reflection data either before or after stationary deconvolution. In addition, numerical test using the 2D synthetic data and field data demonstrates that the match filter has the potential to identify the localized low Q zone of the subsurface from surface reflection data for a layered medium.

ACKNOWLEDGEMENTS

We would like to thank the sponsors of CREWES project for their financial support.

REFERENCES

Aki K. and Richard P. G., 1980, Quantitative Seismology, W. H. Freeman and Co., San Fransisco.

Bath, M., 1974, Spectral analysis in geophysics: Developments in Solid Earth Geophysics, Vol 7, Elsevier Science Publishing Co.

Cheng, P., and Margrave, G. F., 2009, Q analysis using synthetic viscoacoustic seismic data: CREWES research report, 21.

Claerbout, J. F., 1976, Fundamentals of geophysical data processing: McGraw – Hill Inc.

Dasgupta, R., and Clark, R. A., 1998, Estimation of Q from surface seismic reflection data: Geophysics, 63, 2120-2128.

Engelhard, L., 1996, Determination of the seismic wave attenuation by complex trace analysis: Geophysical Journal International, 125, 608-622.

Futterman, W. I., 1962, Dispersive body waves: J. Geohys. Res., 67, 5279-5291.

Hackert, C. L., and Parra, J. O., 2004, Improving Q estimates from seismic reflection data using well-log-based localized spectral correction: Geophysics, 69, 1521-1529.

Hauge, P. S., 1981, Measurements of attenuation from vertical seismic profiles: Geophysics, 46, 1548-1558.

Margarve G. F., 1998, Theory of nonstationary linear filtering in the Fourier domain with application to time-variant filtering: Geophysics, 63, 244-259

Neep, J. P., Sams, M. S., Worthington, M. H., and O'Hara-Dhand, K. A., 1996, Measurement of seismic attenuation from high-resolution crosshole data: Geophysics, 61, 1175-1188.

Park, J., Lindberg, C. R., and Vernon III, F. L., 1987, Multitaper spectral analysis of high frequency seismograms: J. Geoph. Res., 92, 12 675-12 684.

Patton, S. W., 1988, Robust and least-squares estimation of acoustic attenuation from well-log data: Geophysics, 53, 1225-1232.

Quan, Y., and Harris, J. M., 1997, Seismic attenuation tomography using the frequency shift method: Geophysics, 62, 895-905.

Raikes, S. A., and R. E. White, 1984, Measurements of earth attenuation from downhole and surface seismic recordings: Geophysical Prospecting, 32, 892-919.

Sheriff, R. E., and L. P. Geldart, 1995, Exploration seismology, 2nd ed.: Cambridge University Press.

Sun, X., X. Tang, C. H. Cheng, and L. N. Frazer, 2000, P- and S- wave attenuation logs from monopole sonic data: Geophysics, 65, 755-765.

Thomson, D. J., 1982, Spectrum estimation and harmonic analysis: Proc. IEEE, 70, 1055-1096.

Tonn, R., 1991, The determination of seismic quality factor Q from VSP data: A comparison of different computational methods: Geophys. Prosp., Vol. 39, 1-27.

White, R. E., 1992, The accuracy of estimating Q from seismic data: Geophysics, 57, 1508-1511.